THE ROLE OF H_3O^+ IN THE CRYSTAL STRUCTURE OF ILLITE

Fernando Nieto[1],*, Marcello Mellini[2], and Isabel Abad[3]

[1] Departamento de Mineralogía y Petrología and IACT, Universidad de Granada, CSIC, Av. Fuentenueva, 18002 Granada, Spain
[2] Dipartimento di Scienze della Terra, Università di Siena, Via Laterina 8, 53100 Siena, Italy
[3] Departamento de Geología, Universidad de Jaén, Campus Las Lagunillas, 23071 Jaén, Spain

Abstract—In spite of decades of research on the subject, the crystal structure of illite is still poorly understood. The purpose of this study was to address this problem by investigating the nature of the interlayer content in illite IMt-2 from Silver Hill, Montana, using analytical transmission electron microscopy (ATEM), thermogravimetry (TG), and X-ray powder diffraction (XRPD) analyses. The ATEM data, together with literature and TG results, yielded the formula $K_{0.70}Na_{0.01}(H_2O)_{0.42}$ $(Al_{1.53}Fe^{2+}_{0.06}Fe^{3+}_{0.19}Mg_{0.28})_{\Sigma=2.06}(Si_{3.44}Al_{0.56})O_{10}(OH)_2$ or, assuming the presence of H_3O^+, $K_{0.69}Na_{0.01}(H_3O)^+_{0.28}(Al_{1.47}Fe^{2+}_{0.06}Fe^{3+}_{0.19}Mg_{0.28})_{\Sigma=1.99}(Si_{3.40}Al_{0.60})O_{10}(OH)_2$. The first formula indicates surplus interlayer and octahedral species, whereas the second shows no excess. The XRPD data were refined by Rietveld techniques, down to an R_p factor of $10.48-13.8\%$. The mineral composition consists largely of illite-$2M_1$, illite-$1M$, and minor quartz. Although the refinement accuracy is limited by the intrinsic poor quality diffraction of the illites, the partially refined model is consistent with the chemical composition; in particular, attempts to introduce octahedral cations in excess of 2 were fruitless. All the results support the simple structural model, by which the illite structure strictly corresponds to a dioctahedral mica with H_3O^+ replacing K. As a consequence, the crystalchemical formula of illites should be calculated on the basis of six tetrahedral plus octahedral cations.

Key Words—Composition, Hydronium, Illite, Water.

INTRODUCTION

The term illite has been used in the clay minerals literature for decades, in most cases without a strict mineralogical meaning. In general, it is applied to dioctahedral mica, present in sediments and recognized by its 10 Å rational series of XRD peaks. The positions do not change significantly after organic treatments, though alkylammonium is an exception to this rule. The most typical illites seem to show significant interlayer deficit (*e.g.* Hower and Mowatt, 1966); hence, according to the International Mineralogical Association (IMA) nomenclature committee, the term illite should be used to designate interlayer-cation-deficient (<0.85 atoms per formula unit, a.p.f.u.) micas (Rieder *et al.*, 1998).

In spite of its abundance and genetic importance, the crystal structure of illite is poorly known, due to its small grain size and defective character. Because of the XRD pattern and composition similar to muscovite and other micas, its structure has been assumed to be that of dioctahedral micas, with an interlayer cation deficit. However, the means by which such a positive charge deficit would be compensated is controversial. Brown and Norrish (1952) proposed that H_3O^+ ions substitute for K^+, filling the interlayer and justifying the usual water excess in illite analyses. Hower and Mowatt (1966) discussed the nature of water and concluded that

it was present as H_2O molecules; an excess of Si of >3 would, in this case, compensate the positive charge deficit of the interlayer.

Gualtieri *et al.* (2008) attempted to refine the illite structure, presenting the structural characterization of an illite-rich mixed-layer illite-smectite from northern Hungary, with predominant $1M$ polytype. Because of the inability of the Rietveld refinement code to reproduce the diffraction effects of disorder, the final fit of the observed pattern was still imperfect. According to the authors, their refined illite-$1M$ structure model, largely based on mica but including the water molecule, was physically sound but still requiring further development, mostly in the tetrahedral sheet geometry and in the location of water.

Rosenberg (2002) presented an alternative hypothesis, by which the end-member illite would not be a disordered, K-deficient muscovite but a stable, ordered structure consisting of muscovite and pyrophyllite (Py) domains; dehydration of I_w, a metastable, compositional end-member containing 'excess' interlayer water would result in the formation of a metastable, disordered, K-deficient mica (I_d) that might recrystallize to form a stable, ordered, Py domain structure (I_o). Such an hypothesis has yet to be supported by direct evidence.

Hydrothermal or metamorphic K-micas are typically alkali deficient. An exact understanding of the real nature of the so-called pyrophyllitic (or illitic) compositional vector is important for geothermobarometric calculations, as the pyrophyllitic end-member is used in various reactions of the chlorite/phengite geothermo-

* E-mail address of corresponding author:
nieto@ugr.es

barometer (Vidal and Parra, 2000), widely used for low-grade metamorphic rocks.

To further advance the knowledge of the illite structure, a combined study is presented here of the illite standard IMt-2 from Silver Hill, using chemical data obtained by ATEM, water content data obtained from thermogravimetry (TG), and Rietveld refinement of XRD data. The sample was chosen as one of the most representative illites, almost free of smectite mixed layering and showing a typical illite chemical composition (see below). The results should be able to clarify the nature of the illite interlayer, with emphasis on the role of water molecules and/or H_3O^+ ions.

METHODS

Sample

The <2 μm fraction of illite IMt-2 from the Source Clays Repository of The Clay Minerals Society was separated by centrifugation. No further chemical treatment was applied during the separation process. The sample was air-dried and disaggregated. Ethylene glycol (EG) solvation was carried out exposing the sample spread in a Petri capsule to EG vapors at 60ºC for 3 days.

A full description of the Cambrian shale IMt-2 from Silver Hill, Jefferson Canyon, Montana, can be found in Hower and Mowatt (1966).

Further characterization was obtained by high-resolution transmission electron microscopy (HRTEM). Lattice images and electron diffraction patterns (Figure 1) reveal that IMt-2 shows all the microstructural features typical of illite: small particle size, even smaller coherently scattering domains, and (001) sub-parallel orientation of the coherent domains, with limited extension along the (001) plane. On the other hand, IMt-2 does not reveal contrast features interpretable as due to other phases, in agreement with the present XRD characterization which indicated that, among illites, the fine fraction of IMt-2 corresponds to an almost totally pure sample, ideal for detailed structural investigation.

Analytical electron microscopy

Lattice images and quantitative chemical analyses were obtained by analytical electron microscopy (AEM) in a transmission electron microscope (TEM − Philips CM20 (STEM) located at the C.I.C., Universidad de Granada), equipped with an EDAX solid-state EDX detector, and operating at 200 kV, with a point-to-point spatial resolution of 2.7 Å. Quantitative AEM analyses were obtained from powders deposited over a holey C-coated Au grid. To avoid contamination, the mono-mineralic character of each grain was checked by selected area electron diffraction (SAED). A small number of analyses was later rejected, none-the-less, due to evident contamination by other mineral phases. Detrital muscovite and biotite grains, with textural features and compositions clearly indicating detrital

origin, were also avoided. Alkali loss is a significant problem in the AEM analysis of clay minerals. Comparison of the analyses obtained for 15 s and 100 s showed that shorter counting times gave improved K reproducibility; therefore, counting times of 15 s were used as a compromise for major alkali analysis (Nieto *et al.*, 1996). Albite, biotite, spessartine, muscovite, olivine, and titanite standards were used to obtain K-factors for the transformation of intensity ratios to concentration ratios following Cliff and Lorimer (1975). The structural formulae of illites were initially calculated on the basis of 22 negative charges, corresponding to the $O_{10}(OH)_2$ a.p.f.u.

Thermogravimetry

The weight loss on heating, from room temperature to 800ºC, at a rate of 10ºC/min, was determined by
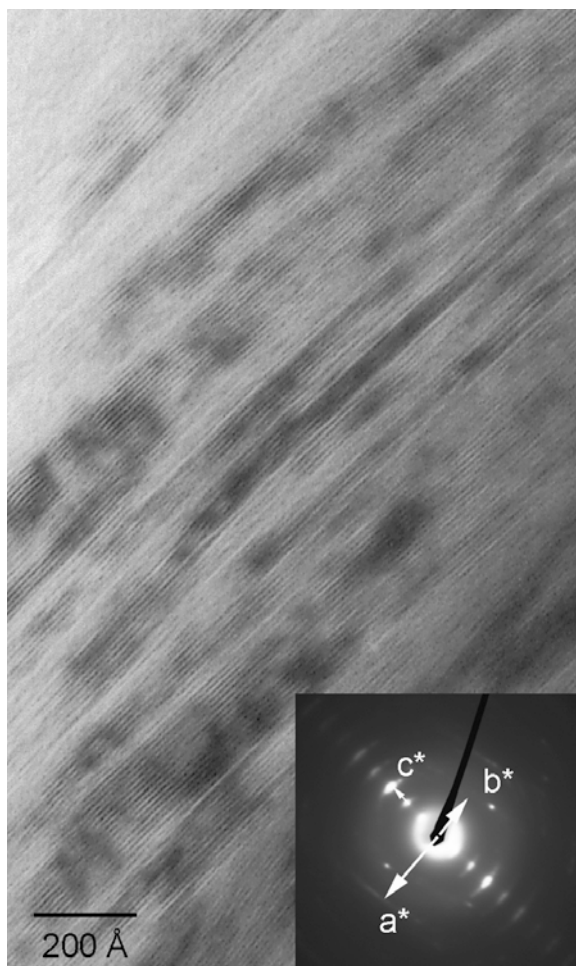

Figure 1. Lattice image and SAED of illite IMt-2 showing domain size and textural characteristics typical of diagenetic illites. The SAED pattern corresponds to that identified as $1M_d$ polytype; due to [001] rotational disorder, it shows diffuse lines the spacing of which corresponds both to (h0l) and (0kl) rows.

differential scanning calorimetry, thermogravimetric analysis (DSC-TGA), using TA Instruments model SDT-Q600 DSC-TGA, equipped with a Pfeiffer Thermostar quadrupole mass spectrometer for the analysis of the volatiles released, on aliquots of ~30 mg of the same illite powders used for TEM and XRD analyses.

XRPD data collection

The patterns were collected using a Bruker D8 Advance diffractometer, with Bragg-Brentano θ/θ geometry, graphite monochromator, and CuKα radiation at 40 kV and 40 mA. Both air-dried and glycolated preparations were scanned in the 3−80º2θ range. The XRPD mounts were prepared carefully by back-loading illite powders into round, 27 mm holders, avoiding any kind of pressure on the sample. Counts were recorded at 0.02º2θ intervals for 30 s. The widths of the various slits were: divergence − 1º, receiving − 0.1º, anti-scatter − 1º; starting from the first observed peak, the values avoid significant beam spilling out of the sample (as experimentally checked using a fluorescent screen). Sample spinning with 15 revolutions/min was used.

No difference was detected between the patterns from air-dried and glycolated samples, with the single exception of a small shoulder in the low-angle region of the 10 Å peak, present in the air-dried sample. The shoulder is present even in highly crystalline micas (*e.g.* Lliang and Hawthorne, 1996) and is probably due to interparticle diffraction (Nadeau *et al.*, 1984).

Rietveld refinement

Refinement was performed using both the FullProf (Rodríguez-Carvajal, 2001) and Topas codes (Coelho, 2000), with slightly different fitting conditions and refining diffraction data from the air-dried and the glycolated sample, respectively.

In both cases, the starting model was built through the progressive introduction of three phases (illite-1*M*, illite-2M_1, quartz). Their initial atomic coordinates were taken from Gualtieri *et al.* (2008), Lliang and Hawthorne (1996), and Levien *et al.* (1980), respectively. Scale factors were repeatedly refined during the fitting procedure. The background was refined using a sixth-order Chebychev polynomial. Preferred orientation was treated using the March-Dollase formula. In most of the trials, the minor quartz was used as an internal standard, to correct for possible diffractometer misalignment or small differences in the surface height of the sample.

The peak shapes were modeled in two different ways, using pseudo-Voigt (FullProf, FP) or Pearson-VII functions (Topas), in both cases, taking into account the variation of full peak width at half-maximum height (FWHM) *vs.* θ. In the final Topas refinement cycles, spherical harmonics described preferred orientation. Isotropic atomic displacement factors were kept fixed at the known values.

RESULTS

Illite chemical composition

Analytical electron microscopy (AEM) results were obtained for various individual grains of illite IMt-2 (Table 1). No systematic differences, possibly related to texture or grain size, were found (after excluding the detrital muscovite and biotite grains, as mentioned above). The compositions were typical of illite, as previously described in the literature and defined by the IMA (Rieder *et al.*, 1998). The AEM results can be summarized as follows. The chemical composition is not

Table 1. Structural formulae* for Silver Hill illites on the basis of TEM/AEM data.

	Si	^{IV}Al	^{VI}Al	Fe	Mg	Σ oct.	K
Imt-2/1	3.44	0.56	1.48	0.28	0.33	2.10	0.66
Imt-2/2	3.41	0.59	1.48	0.30	0.28	2.06	0.76
Imt-2/3	3.38	0.62	1.52	0.25	0.35	2.11	0.68
Imt-2/4	3.43	0.57	1.58	0.23	0.28	2.09	0.63
Imt-2/6	3.44	0.56	1.66	0.16	0.24	2.05	0.67
Imt-2/7	3.63	0.37	1.52	0.28	0.26	2.05	0.53
Imt-2/12	3.34	0.66	1.57	0.23	0.27	2.07	0.76
Imt-2/13	3.45	0.55	1.51	0.26	0.35	2.12	0.58
Imt-2/14	3.33	0.67	1.54	0.28	0.26	2.08	0.74
Imt-2/16	3.44	0.56	1.45	0.25	0.37	2.07	0.76
Imt-2/20	3.40	0.60	1.55	0.26	0.26	2.08	0.69
Imt-2/22	3.63	0.37	1.63	0.19	0.19	2.01	0.56
Imt-2/23	3.28	0.72	1.54	0.24	0.28	2.06	0.87
Imt-2/24	3.68	0.32	1.65	0.17	0.17	2.00	0.54
Imt-2/25	3.43	0.57	1.43	0.28	0.32	2.03	0.86
Imt-2/26	3.35	0.65	1.49	0.30	0.27	2.06	0.80
Imt-2/27	3.42	0.58	1.48	0.26	0.30	2.04	0.81

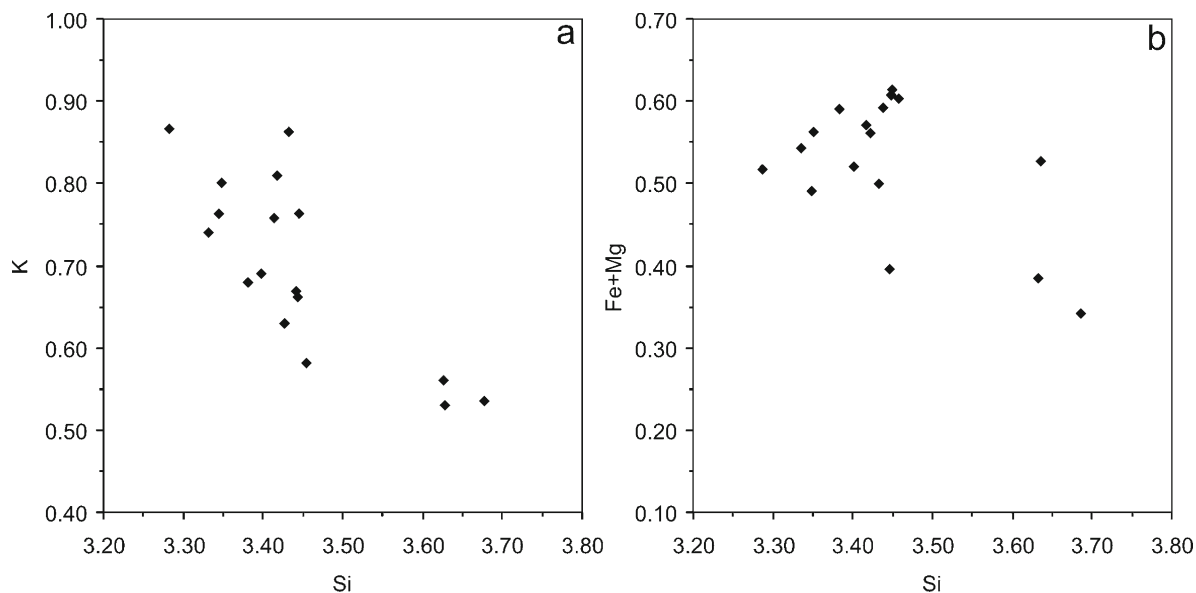* Normalized to $O_{10}(OH)_2$ and considering 76% of Fe as Fe^{3+} and 24% as Fe^{2+}.

Figure 2. AEM data for individual particles of the IMt-2 sample.

homogeneous at the sample scale, changing from grain to grain (Figure 2). The Si content ranges from 3.28 to 3.68 a.p.f.u. The sum (Fe + Mg) ranges from 0.34 to 0.62, with most of the values between 0.5 and 0.6 a.p.f.u. The K content ranges from 0.53 to 0.87 a.p.f.u. K and Si are coarsely negatively correlated (Figure 2). After normalization on 11 oxygens p.f.u., the octahedral sum is systematically >2, with an average value of 2.06 a.p.f.u. Ca, Na, Mn, and Ti are absent or below the detection limit of the technique. The IMt-2 illite composition is very similar to that obtained by Hower and Mowatt (1966) on various granulometric fractions (<0.5 μm) of the sample, with the exception of the Si/Al ratio (Table 2). The two sets of data are complementary. The AEM composition is *in situ* and therefore basically free of contamination, but lacks data for H_2O and Fe^{3+}/Fe^{2+} and is unable to measure small quantities of

Na accurately. All of the missing data are present in the Hower and Mowatt bulk analyses. Therefore a combination of the two sets of data has been used to obtain the most likely estimate of the IMt-2 illite composition. The difference regarding Si estimates is due to the presence of quartz even in the fine fractions, as recognized both during the TEM sessions and the Rietveld analysis (see later), and in agreement with other researchers who previously studied the same sample (*e.g.* Gailhanou *et al.*, 2007). An average formula has been calculated using the AEM data for Si, Al, total Fe, Mg, and K (the last three elements being virtually equal to those of Hower and Mowatt, 1966), combined with those of Hower and Mowatt (1966) for H_2O, Fe^{3+}/Fe^{2+} ratio, and Na (formulae A and B in Table 2).

Starting from 6.4 wt.% H_2O determined by Hower and Mowatt (1966), the H content has been estimated to

Table 2. Chemical data of Silver Hill illites.

	SiO_2	Al_2O_3	Fe_2O_3	FeO	MgO	TiO_2	K_2O	CaO	Na_2O	H_2O^-	H_2O^+	Total
Chemical composition in oxides (wt.%)*												
	55.1	22	5.28	1.34	2.8	0.63	8.04	0.02	0.08	1.0	6.4	102.69

	Si	^{IV}Al	^{VI}Al	Fe^{3+}	Fe^{2+}	Mg	Σoct.	K	Na			
Structural formulae per 11 oxygens*												
	3.66	0.34	1.38	0.26	0.07	0.28	1.99	0.68	0.01			

Average structural formula of IMt-2 illites analyzed by TEM/AEM and assuming the water reported by Hower and Mowatt (1966)

	Si	^{IV}Al	^{VI}Al	Fe^{3+}	Fe^{2+}	Mg	Σoct.	K	Na	H_2O	H_3O^+	Σinter.
A	3.44	0.56	1.53	0.19	0.06	0.28	2.06	0.70	0.01	0.42		1.13
B	3.40	0.60	1.47	0.19	0.06	0.28	1.99	0.69	0.01		0.28	0.98

* (taken from Hower and Mowatt, 1966)

be 2.85 a.p.f.u., with 2.0 corresponding to the OH in the octahedral sheet and the remaining 0.85 allocated to the interlayer. The latter value may represent 0.42 water molecules p.f.u. or, alternatively, 0.28 H_3O^+. The first alternative would represent a clear excess of interlayer positions over the available 0.3 sites not occupied by K and Na. By the second alternative, the sum of K, Na, and H_3O^+ would be 0.98 a.p.f.u., corresponding exactly to complete occupancy of the interlayer.

The charge difference between H_3O^+ and H_2O has an effect on the calculation of the rest of the formula. Assuming neutral water, the illite formula would be calculated in the traditional way, on the basis of 11 oxygens (row A in Table 2). Assuming H_3O^+, the remaining cations diminish (row B in Table 2). Consequently, the excess Si over 3 a.p.f.u. is not far from the sum Mg + Fe^{2+} (*i.e.* Tschermaks/phengitic substitution) and octahedral population becomes quite stoichiometrically dioctahedral.

Thermogravimetry

A typical TG pattern for illite IMt-2 is reported (Figure 3). After an initial weight loss of 2.79 wt.% at temperatures of <138ºC, the remaining total weight loss is 6.86 wt.%. The TG curve has a relatively constant slope, with two maximum emissions at 263ºC and 556−658ºC, corresponding to ~1.5 and 5.4 wt.%, respectively. The first peak can be interpreted as due to water loss from the interlayer (0.85 H, see above) and the second one to layer dehydroxylation (2.00 H).

According to the quadrupole mass spectrometer, the most important mass/charge ratios are 18 and 17, with small signals (approximately two orders of magnitude lower) at 44; therefore, the weight loss has been interpreted as largely due to water-related species (H_2O and OH) plus very minor CO_2. In conclusion, the current TG data support the previous interpretation, based on the Hower and Mowatt data.

As far as the 263ºC water release is concerned, this feature apparently escaped from identification during the previous studies reporting TG-DTG determinations, possibly because it was spread over a wider temperature range in illites with larger disorder features and containing smectite layers. The water released at temperatures >600ºC might indicate the presence of *cis*-vacant sites, in addition to the *trans*-vacant sites dehydroxylating at temperatures of <600ºC, as suggested by Drits and Zviagina (2009).

Rietveld refinements

The main results of three different refinements, under different conditions or with different levels of completeness are reported (Table 3). FP302 (made by FullProf) assumes fixed structure models and refines only the profile parameters, unit cells, and modal composition, using data from the air-dried sample. The FP304 trial also attempted the atomic parameters refinement, with limited success in terms of derived bond geometry. The two trials refined to apparently satisfactory levels (*i.e.* R_p values of 13.8 and 11.7%, respectively) and produced similar mineralogical compositions (dominant illite-$2M_1$, 81 wt.%; illite-$1M$, 14 wt.%; minor quartz, 5 wt.%). The kind of fit achieved is shown for the FP304 pattern (Figure 4); note the overall similarity with figure 4b in Gualtieri *et al.* (2008).

Better R_p values could be obtained using Topas, under similar fitting conditions but introducing spherical harmonics in the description of preferred orientation. For instance, the best Topas refinement (Figure 5) produced R_p of 10.48%. During this refinement, attempts to introduce further atoms within the vacant octahedral site ($M1$) were fruitless, both in the $1M$ and $2M_1$
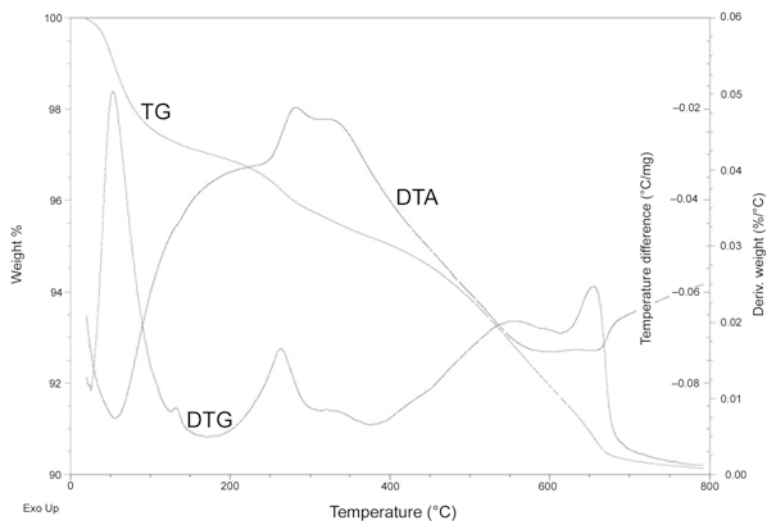

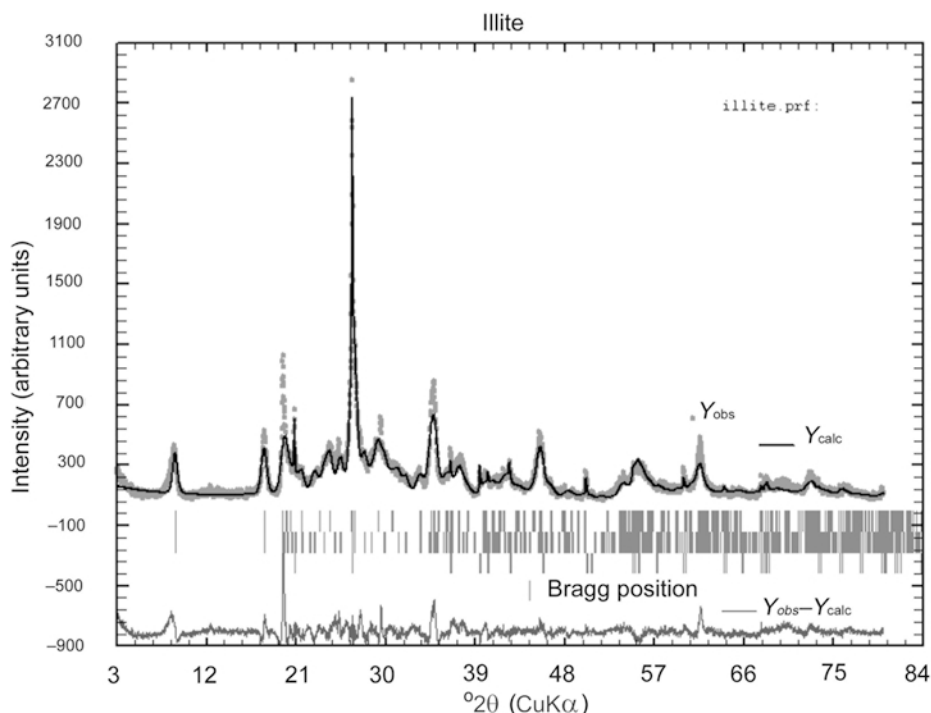Figure 3. TG, DTG, and DTA plots for illite IMt-2.

Figure 4. Graphical output of the FP304 FullProf Rietveld refinement. Air-dried sample. Observed, calculated, and difference curves are reported.

structures, indicating that the site was empty, as expected for a *trans*-vacant structure. The Topas refinement produced estimates of the mineralogical composition different from those of FullProf (Table 3). Illite-$2M_1$ is still the dominant phase, but decreases to 46 wt.%; conversely, illite-$1M$ increases to 37 wt.%; quartz also increases, to 17 wt.%. Nevertheless, the $1M/2M_1$ ratio could be biased by strong correlation problems and by the presence of partial *cis-vacant* replacement (Drits and Zviagina, 2009).

Also for Topas, the derived bond geometries were unsatisfactory. In particular, illite-$1M$ and quartz produced apparently reliable bonding patterns, whereas illite-$2M_1$ led to unreliable distances (*e.g.* $K-O5$ as short as 2.2 Å; tetrahedral distances as long as 2.2 Å, in the cases of $T2-O3$ and $T1-O4$, respectively). Therefore atomic parameters were finally kept unrefined at the literature values.

The intrinsically limited accuracy of the illite refinements, testified by current data and those of Gualtieri *et al.* (2008), suggests care in the interpretation of other potentially important parameters, such as the occupancy factors of the K and M sites reported in Table 3.
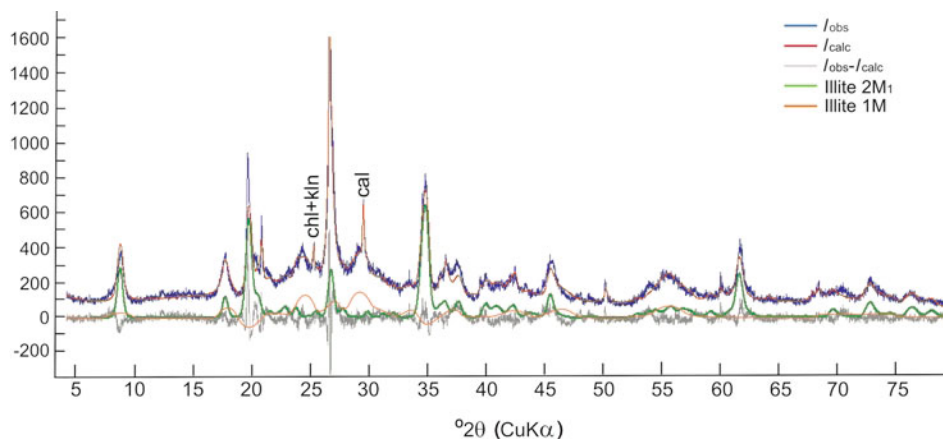

Figure 5. Graphical output of the Topas Rietveld refinement. EG-solvated sample. Observed, calculated, and difference curves are reported. Atomic coordinates are from the literature (see text for explanation).

DISCUSSION AND CONCLUSIONS

Limits of the Rietveld refinement of illite

Several features combine to make difficult or impossible the Rietveld refinement of poorly crystalline materials such as illite. One such first feature is the small crystal size. A second obstacle arises from the soft nature of illite flakes which easily undergo deformation during geological history and subsequent handling. The curved character of the crystals is also inherited from the original texture of the parent smectite (Abad *et al.*, 2003). In conclusion, low, wide diffraction peaks are produced, with intensities spread out over wide θ ranges. Several structural faults (*e.g.* polytypic stacking faults) further reduce the size of the coherent scattering domain to nanometric values. Finally, the broadening effect for a flake will be anisotropic, affecting the different diffractions in different ways.

The current refinement is, therefore, difficult to improve. Much information is contained in the XRPD, though heavily degraded.

The Rietveld refinement of illite IMt-2 indicated that the specimen consists of illite-2M_1, illite-1M, and quartz.

Very minor amounts of calcite, feldspars, and chlorite produced small, recognizable XRPD peaks. These indications match the data obtained for illite IMt-2 by Gailhanou *et al.* (2007).

Therefore, 83−95 wt.% of the specimen consists of the flat 2:1 layers present in the starting models (illite-1M of Gualtieri *et al.*, 2008; muscovite 2M_1 of Lliang and Hawthorne, 1996). Other important parameters, such as the interlayer occupancy, or the vacant nature of the M1 site, may not be sharply defined when using only the Rietveld results.

The nature of the 1M_d illite polytype

Literature dealing with diagenetic environments traditionally describes a progressive change in the nature of the illite polytype with diagenetic grade, based on XRPD identification (Frey, 1987). Pure diagenetic illites are of the so-called 1M_d polytype, which progressively evolves toward 2M_1. Intermediate stages show peaks corresponding to 1M and 2M_1, often interpreted as a progressive 1M_d → 1M → 2M_1 sequence. Low-grade metamorphic micas are only 2M_1, showing an X-ray pattern equivalent to that of higher-metamorphic-grade

Table 3. Selected Rietveld refinement results (disagreement factors R_{wp}, R_p, and R_{exp}; lattice parameters; site occupancies) for illite IMt-2.

	FP302	FP304	Topas
R_{wp} (%)	18	15.2	13.17
R_p (%)	13.8	11.7	10.48
R_{exp} (%)	6.97	6.97	7.62
Illite-1M			
a (Å)	5.212	5.198	5.235
b (Å)	9.062	9.058	9.012
c (Å)	10.173	10.175	10.134
β (º)	101.8	101.72	101.35
Wt.%	13.5	14.3	36.78
R_{bragg} (%)	15.7	8.56	6.39
K site	1 K	1 K	1 K
M site	1 Al	0.97 Al*, 0.03 Fe	0.9 Al*, 0.1 Fe
Illite-2M_1			
a (Å)	5.222	5.22	5.222
b (Å)	9.043	9.037	9.037
c (Å)	20.034	20.035	20.061
β (º)	95.81	95.9	95.67
Wt.%	80.7	81.1	46.12
R_{bragg} (%)	13.6	9.17	7
K site	1 K	0.71 K	0.97 K, 0.03 O
M site	1 Al	0.7 Al*, 0.3 Fe	0.8 Al, 0.2 Mg
Quartz			
a (Å)	4.916	4.916	4.916
b (Å)	4.916	4.916	4.916
c (Å)	5.405	5.405	5.405
Wt.%	5.8	4.6	17.1
R_{bragg} (%)	7.2	7.6	3.81

Al*-Al atomic factor, used for light cations. Proportion equivalent to Al + Mg.
FP302 and FP304 are FullProf refinements, carried out using fixed and variable atomic coordinates, respectively. The Topas refinement was done using fixed atomic coordinates.

muscovites or igneous muscovites. Accordingly, the proportion of the two polytypes has been used as a grade criterion (Merriman and Peacor, 1999). In SAED, $1M_d$ polytype is identified based on the absence of discrete non-basal reflections (Figure 1) and $2M_1$ polytype on a regular pattern consistent with a 20 Å $C2/m$ structure. Nevertheless, a $1M$ polytype has seldom been identified in the plethora of TEM images of diagenetic/low-grade metamorphic samples, the few exceptions being restricted to particular, Mg-rich, chemical compositions (Peacor *et al.*, 2002). Dong and Peacor (1996) concluded that the $1M$ polytype was not an intermediate step in the polytype evolution.

The IMt-2 sample has been refined as a mixture of major $2M_1$ and minor $1M$ polytypes. Gualtieri *et al.* (2008) refined a less evolved sample, which still contained smectite layers, using only the $1M$ polytype structure. Such a difference is consistent with the progressive development of $2M_1$ layers.

Chen and Wang (2007) presented images that were sub-atomic in resolution, interpreted by image simulation as intergrown $1M$ and $2M_1$ illite polytypes. The laterally consistent $1M$ and $2M_1$ illite domains were aligned along the same orientation and were crystallographically continuous, normal to c^*. The interlayer-stacking angle changed in a series of successive layers as a consequence of intralayer stepwise changes. According to this model the two polytypes coexist within the same domain as randomly faulted sequences.

The present authors agree with that interpretation, and conclude that the $1M_d$ polytype results from the fine intergrowth of the two polytypes. Such a model explains the simultaneous presence in XRPD of reflections corresponding to $1M$ and $2M_1$ illite, the change of their ratio with the diagenetic evolution, and the typical character of $1M_d$ SAED (Figure 1).

The real nature of illitic substitution

Metamorphic micas are usually interpreted as showing octahedral sums greater than 2 and interlayer populations of <1. Deficit in positive interlayer charge would be compensated in part by the octahedral excess, and in part by excess of Si over the theoretical Tschermaks substitution. According to previous calculations, these two chemical features are derived from the omission of unconventional, often not-analyzed positive cations such as H_3O^+ and/or NH_4^+ (Nieto, 2002). By introducing the original data of Hower and Mowatt (1966) or the new consistent TG values, the IMt-2 structural formula may be calculated, producing full occupancy of the interlayer by K^+ and H_3O^+. Furthermore, the octahedral composition achieves the theoretical value of 2 nicely. In conclusion, the exchange vector characterizing illites is $K_{-1}H_3O^+$, rather than $SiAl_{-1}$, K_{-1}.

The meaning of excess water in illite has been similarly discussed by Drits and McCarty (2007), who interpreted their heating experiments in terms of the release of H_2O molecules from the interlayer. The exchange vector $K_{-1}H_3O^+$ had previously been invoked to explain excess H_2O contents in micas (Guidotti and Dyar, 1991).

The normalization of dioctahedral mica formulae. The normalization of formulae of minerals with solid solution series is a controversial matter as some crystal-chemical assumptions need to be accepted. In most cases, such assumptions are not a general rule; hence a mineral formula is always an approximation. The mica case is particularly complex as *in situ* analyses lack some significant data, namely H, N, Li, or Fe^{2+}/Fe^{3+} ratio and all of these data may affect the final formula.

Mica formulae are usually calculated on the basis of $O_{10}(OH)_2$ a.p.f.u., which, in practice, is equivalent to 22 negative charges, due to the lack of information about water content. The calculated factor for the normalization depends, therefore, on the assumption of a given Fe^{2+}/Fe^{3+} ratio and is inevitably affected by the lack of data about some positive cations. As H_3O^+ and NH_4^+ cannot be routinely determined, the overall calculated positive charge is smaller than the real one and the rest of the cations are artificially overestimated, producing octahedral sums >2.

The present data suggest that the real occupancy of the octahedral sheet is actually very close to 2, if the excess water is assumed to fill the interlayer sites in the form of H_3O^+ (Table 2). Appropriate normalization may necessitate fixing of the sum of tetrahedral and octahedral cations to six, thereby also allowing the calculation of Fe^{2+}/Fe^{3+}, if one positive charge is assumed for the interlayer.

Consequences for geothermobarometry. One of the fundamental reasons for the current limited knowledge of the transitional field between diagenesis and metamorphism has been the lack of adequate grade criteria for clastic materials. There are no mineral changes in pelitic and psammitic rocks, over a 200ºC temperature range, from the disappearance of kaolinite and interstratified smectite to the biotite isograd. Therefore, geothermobarometry, based on mica/chlorite local equilibrium (Vidal and Parra, 2000; Parra *et al*., 2002), has been used widely for low-grade metamorphic rocks and is proposed to be extended to still lower grades.

Illitic substitution is a significant component in low-temperature micas (Abad *et al.*, 2006). Pyrophillitic substitution ($SiAl_{-1}$, K_{-1}) is, therefore, currently considered in mica/chlorite geothermobarometry and some of the calculated reactions include the pyrophillitic term. Nevertheless, according to the present results, the nature of illitic substitution is different and consequently the thermodynamic properties used for its calculation should be changed. In addition, the proposed change in the normalization criteria would affect the other compo-

nents. In particular, an approximate value could be calculated for Fe^{3+}, which is still a challenge in the application of this geothermobarometric approach.

The real nature of illitic substitution $(K_{-1}H_3O^+)$ and consequences for the normalization of the mica formula may constitute significant contributions to be further taken into account in the extension of the mica/chlorite geothermobarometry to very low metamorphic grade.

All of the data favor the hypothesis of Brown and Norrish (1952), namely, full occupancy of the interlayer by alkaline (mostly K^+) and hydronium (H_3O^+) cations. The illite crystal structure closely corresponds to the dioctahedral micas, with replacement of K^+ by H_3O^+.

ACKNOWLEDGMENTS

REFERENCES

Abad, I., Nieto, F., Peacor, D.R., and Velilla, N. (2003) Prograde and retrograde diagenetic and metamorphic evolution in metapelitic rocks of Sierra Espuña (Spain). *Clay Minerals*, **38**, 1−23.

Abad, I., Nieto, F., Gutierrez-Alonso, G., Do Campo, M., Lopez-Munguira, A., and Velilla, N. (2006) Illitic substitution in micas of very low-grade metamorphic clastic rocks. *European Journal of Mineralogy*, **18**, 59−69.

Brown, G. and Norrish, K. (1952) Hydrous micas. *Mineralogical Magazine*, **29**, 929−932.

Chen, T. and Wang, H.J. (2007) Determination of layer stacking microstructures and intralayer transition of illite polytypes by high-resolution transmission electron microscopy (HRTEM). *American Mineralogist*, **92**, 926−932.

Cliff, G. and Lorimer, G.W. (1975) The quantitative analysis of thin specimens. *Journal of Microscopy*, **103**, 203−207.

Coelho, A.A. (2000) Whole-profile structure solution from powder diffraction data using simulated annealing. *Journal of Applied Crystallography*, **33**, 899−908.

Dong, H. and Peacor, D.R. (1996) TEM observations of coherent stacking relations in smectite, I/S and illite of shales: evidence for MacEwan crystallites and dominance of $2M_1$ polytypism. *Clays and Clay Minerals*, **44**, 257−275.

Drits, V.A. and McCarty, D.K. (2007) The nature of structure-bonded H_2O in illite and leucophyllite from dehydration and dehydroxylation experiments. *Clays and Clay Minerals*, **55**, 45−58.

Drits, V.A. and Zviagina, B.B. (2009) *Trans*-vacant and *cis*-vacant 2:1 layer silicates: structural features, identification and occurrence. *Clays and Clay Minerals*, **57**, 405−415.

Frey, M. (1987) Very low-grade metamorphism of clastic sedimentary rocks. Pp. 9−58 in: *Low-temperature Metamorphism* (M. Frey, editor). Blackie, Glasgow, UK.

Gailhanou, H., van Miltenburg, J.C., Rogez, J., Olives, J.,

Amouric, M., Gaucher, E.C., and Blanc, P. (2007) Thermodynamic properties of anhydrous smectite MX-80, illite IMt-2 and mixed-layer illite-smectite ISCz-1 as determined by calorimetric methods. Part I: Heat capacities, heat contents and entropies. *Geochimica et Cosmochimica Acta*, **71**, 5463−5473.

Gualtieri, A.F., Ferrari, S., Leoni, M., Grathoff, G., Hugo, R., Shatnawi, M., Paglia, G., and Billinge, S. (2008) Structural characterization of the clay mineral illite-$1M$. *Journal of Applied Crystallography*, **41**, 402−415.

Guidotti, C.V. and Dyar, M.D. (1991) Ferric iron in metamorphic biotite and its petrologic and crystallochemical implications. *American Mineralogist*, **76**, 161−175.

Hower, J. and Mowatt, T.C. (1966) Mineralogy of illites and mixed-layer illite/montmorillonites. *American Mineralogist*, **51**, 825−854.

Levien, L., Prewitt, C.T., and Weidner, D.J. (1980) Structure and elastic properties of quartz at pressure. *American Mineralogist*, **65**, 920−930.

Lliang, J.J. and Hawthorne, F.C. (1996) Rietveld refinement of micaceous materials: muscovite-$2M_1$, a comparison with single-crystal structure refinement. *The Canadian Mineralogist*, **34**, 115−122.

Merriman, R.J. and Peacor, D.R. (1999) Very low-grade metapelites: mineralogy, microfabrics and measuring reaction progress. Pp. 10−60 in: *Low-grade Metamorphism* (M. Frey and D. Robinson, editors). Blackwell Science, Oxford, UK.

Nadeau, P.H., Wilson, M.J., McHardy, W.J., and Tait, J.M. (1984) Interparticle diffraction: a new concept for interstratified clays. *Clay Minerals*, **19**, 757−769.

Nieto, F. (2002) Characterization of coexisting NH_4- and K-micas in very low-grade metapelites. *American Mineralogist*, **87**, 205−216.

Nieto, F., Ortega-Huertas, M., Peacor, D., and Arostegui, J. (1996) Evolution of illite/smectite from early diagenesis through incipient metamorphism in sediments of the Basque-Cantabrian Basin. *Clays and Clay Minerals*, **44**, 304−323.

Parra, T., Vidal, O., and Agaard, A. (2002) A thermodynamic model for Fe-Mg dioctahedral K white micas using data from phase-equilibrium experiments and natural pelitic assemblages. *Contributions to Mineralogy and Petrology*, **143**, 706−732.

Peacor, D.R., Bauluz, B., Dong, H., Tillick, D., and Yan, Y. (2002) Transmission and analytical electron microscopy evidence for high Mg contents of $1M$ illite: Absence of $1M$ polytypism in normal prograde diagenetic sequences of pelitic rocks. *Clays and Clay Minerals*, **50**, 757−765.

Rieder, M., Cavazzini, G., D'Yakonov, Y.S., Kamanetskii, V.A.F., Gottardi, G., Guggenheim, S., Koval, P.K., Müller, G., Neiva, A.M.R., Radoslovich, E.W., Robert, J.L., Sassi, F.P., Takeda, H., Weiss, Z., and Wones, D.R. (1998) Nomenclature of the micas. *The Canadian Mineralogist*, **36**, 1−8.

Rodríguez-Carvajal, J. (2001) *An introduction to the program FullProf2000*, version 2.00, January 2004.

Rosenberg, P.E. (2002) The nature, formation, and stability of end-member illite: A hypothesis. *American Mineralogist*, **87**, 103−107.

Vidal, O. and Parra, T. (2000) Exhumation paths of high-pressure metapelites obtained from local equilibria for chlorite-phengite assemblages. *Geological Journal*, **35**, 139−161.